Studies of large, non-circular, reversed field pinch discharges



1987 Nucl. Fusion 27 1795

(http://iopscience.iop.org/0029-5515/27/11/005)

# STUDIES OF LARGE, NON-CIRCULAR, REVERSED FIELD PINCH DISCHARGES

A. ALMAGRI, S. ASSADI, R.N. DEXTER,
S.C. PRAGER, J.S. SARFF, J.C. SPROTT
Department of Physics,
University of Wisconsin,
Madison, Wisconsin,
United States of America

ABSTRACT. Reversed field pinch (RFP) discharges have been produced in a large (1.39 metre major radius, 0.56 metre average minor radius), thick walled (5 cm), aluminium vacuum vessel with indented sides. The discharges are self-reversed and ramped up to a current of 300 kA over a time of 10 ms. Reversal is sustained for $\gtrsim 10$ resistive diffusion times, despite the presence of large magnetic fluctuations. The influence of the bad poloidal magnetic curvature on RFP stability is examined by measurement of magnetic fluctuations near the plasma edge in the separate bad and good curvature regions of the non-circular plasma for RFP and non-reversed discharges with an edge safety factor, $q_a$, of 0.4 and 1.4. For $q_a \sim 1.4$ discharges, the poloidal field curvature is small. The large device size permits RFP startup at a low toroidal loop voltage ($\lesssim 200$ V), which is applied to a gap exposed to plasma, but successfully protected against arcing (up to 300 V). RFP plasmas have also been obtained with a toroidal limiter.

## 1. INTRODUCTION

Most reversed field pinch (RFP) experiments have been carried out on devices of relatively small size and circular cross-section [1]. Exceptions are the old, large, British Zeta device [2] and the recent, vertically elongated Multipinch [3]. Most RFP devices employ a conventional design in which a thin, resistive, metallic vacuum liner is surrounded by a close fitting, thick, highly conducting shell, which in turn is surrounded by toroidal field windings and axisymmetric equilibrium field and Ohmic heating coils.

Operation of a large (0.56 m average minor radius), non-circular RFP with many unconventional features has allowed the study of several RFP physics and operations issues. The midplane indentation of the conducting wall provides a non-circular plasma as shown in Fig. 1, which also shows a numerically calculated, magnetic flux plot for an RFP plasma. We report here the equilibrium properties of such RFP plasmas sustained for many resistive diffusion times. We also have explored the influence of magnetic curvature on plasma fluctuations. The variable curvature that accompanies the non-circular cross-section, as noted in Fig. 1, affords the opportunity to compare magnetic fluctuations in regions of local bad poloidal curvature with regions of local good curvature

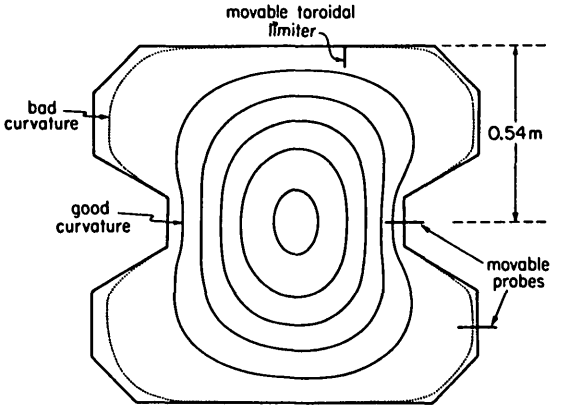


*FIG. 1. Numerically computed poloidal magnetic flux plot. Regions of good curvature (midplane) and bad curvature are noted. The major radius is 1.39 m.*

(the midplane). The role of bad curvature of the poloidal magnetic field (and the contribution of pressure driven instabilities to turbulent fluctuations) is more difficult to discern in circular RFPs which contain uniform bad curvature over the entire cross-section. To further alter the magnetic curvature for comparative studies of fluctuations, we have also operated the

device as a non-reversed pinch with edge safety factors, $q_a$, of 0.4 and 1.4. For the tokamak-like latter case, the toroidal field curvature becomes dominant, and any poloidal curvature effects observed in the low-q cases should be greatly diminished.

Two operations goals successfully demonstrated are low voltage startup ($\lesssim$200 V) permitted by the large size (low resistance), and protection of high voltage electrical gaps (up to 300 V at startup) exposed to the plasma. Finally, RFP plasmas have been sustained with a movable toroidal limiter within the vacuum chamber. After a brief machine description (Section 2), we describe general discharge characteristics in Section 3, fluctuation studies in Section 4, and movable limiter results in Section 5. Section 6 contains concluding remarks.

## 2. MACHINE DESCRIPTION

The decommissioning of the Wisconsin Levitated Octupole [4] provided a large (1.39 metre major radius, 0.56 metre average minor radius), thick walled (5 cm), aluminium vacuum vessel with wall indentations whose original function was to relieve the magnetic forces on the internal rings which were removed for the purpose of this experiment. It was a relatively simple task to reconfigure the device to operate as an RFP, low field tokamak, or non-reversed pinch. As an RFP the device is unconventional, not only in its large size and non-circular cross-section, but also in the fact that the vacuum vessel serves the function of liner, conducting shell, and toroidal and equilibrium field coils. The toroidal field is produced by currents in the vessel wall, and the poloidal fields are driven by a 16-turn primary winding on the 2.0 V·s iron core.

One implication of this design is that insulated voltage gaps are exposed to the plasma, and thus a combination of low voltage startup and special gap protection is required to prevent arcing. The poloidal field gap (i.e. the cut the short way around) is protected with a 20 cm wide strip of ceramic, and startup voltages are typically $\lesssim$200 V. Several versions of poloidal field gap protection were unsuccessful and exhibited serious arcing. The final version was successful, and had the following features: The vacuum seal at the poloidal gap was formed of Viton, 6 mm thick. This was permitted to extend 1 cm into the plasma region so as to form the fundamental gap insulator. The Viton was protected from plasma by tightly fitting, high density polyethylene fixtures at sides and top. The sides were protected by stainless steel limiters, and overall was a 20 cm wide strip of ceramic. No problems were experienced with startup voltages, typically, in the 200–300 V range.

A typical RFP discharge is initiated by filling the device with 0.1–0.2 millitorr of $H_2$ about 70 ms before the pulse. A toroidal field of $\sim$600 G on axis is applied and crowbarred. A cw microwave source of $\sim$50 W at 2.45 GHz is used to produce a low density, electron cyclotron heated plasma for preionization. When the toroidal field has decayed to a value in the range of 100–200 G, a capacitor bank of 0.048 F charged typically to 4.4 kV is then discharged into the 16-turn poloidal field winding through a 430 $\mu$H inductor whose function is to smooth the plasma current waveform and limit the current in the event of a gap arc or saturation of the iron core.

The machine contains two sources of large magnetic field error. At the poloidal gap, a radial magnetic field exists which is, at least, the order of the equilibrium field. The dominant poloidal mode number is m = 4, and the toroidally localized perturbation produces a broad toroidal mode number spectrum. A manhole in the top of the vacuum vessel is covered with a 2 cm thick aluminium plug electrically connected (via electrical joint compound) to the vessel. The residual field error has a spatial extent about equal to the hole size (40 cm × 28 cm) and with a magnitude of $\sim$10% of the equilibrium field at a distance of 15 cm below the hole.

## 2. DISCHARGE CHARACTERISTICS

The time dependence of various electrical and plasma quantities for a typical 300 kA RFP discharge is shown in Fig. 2. The plasma current $I_p$ as measured by a Rogowski loop just inside the vacuum vessel is seen to ramp up to its maximum value over a time of about 10 ms as in other devices [5]. Concurrent with this, the average toroidal field $\langle B_T \rangle$ as measured by a flux loop just inside the vacuum vessel ramps up to a value approaching 500 G. The toroidal field at the wall, $B_{Tw}$, as determined from the poloidal current in the vessel wall self-reverses after 2–3 ms and remains reversed for about 10 ms. The loop voltage on axis is determined from the poloidal field gap voltage $V_{pg}$ by using the relation

$$V_\ell = V_{pg} - 0.44\,(1 + 3.3\theta^2)\,dI_p/dt \qquad (1)$$

For a large aspect ratio, circular plasma of minor radius a, the field reversal parameter F and the pinch

parameter $\theta$ are, respectively, given by

$$F = B_{Tw}/\langle B_T \rangle \tag{2}$$

and

$$\theta = B_{pw}/\langle B_T \rangle = \mu_0 I_p/2\pi a \langle B_T \rangle \tag{3}$$

where $B_{pw}$ is the poloidal field at the wall. For the non-circular plasma of low aspect ratio, we choose two analogous parameters, which would completely describe the plasma if $\lambda$ (= J/B) were constant in space. For our purposes, we take $\langle B_T \rangle$ as the toroidal flux divided by the cross-sectional area of the vacuum vessel and $B_{Tw}$ as the toroidal field at the wall at a major radius such that F = 1 when $I_p = 0$. Theta is defined by analogy with Eq. (3) as

$$\theta = \mu_0 I_p/\ell \langle B_T \rangle \tag{4}$$

where $\ell = 4.89$ m is the distance around the vacuum vessel wall in the poloidal direction. These definitions give a predicted F–$\theta$ curve for $\lambda$ = const that is similar to the Bessel function model for a cylindrical plasma [6].

The plasma density shown in Fig. 2 is from a Langmuir probe at the edge of the plasma and is indicated in arbitrary units. The arbitrary units are approximately $10^{10}$ cm$^{-3}$. Data from the 70 GHz interferometer were not available for this shot, but on similar discharges the line averaged density along the vertical midcylinder is about 1000 times larger than the edge density with a similar time dependence. The conductivity temperature (in eV) is determined from the plasma current and loop voltage assuming Spitzer resistivity [7] with a constant current profile and Z = 1 according to

$$T_\sigma = 0.0363\ (fI_pR_0/AV_\ell)^{2/3} \tag{5}$$

where $R_0$ is the major radius (1.39 m), A is the cross-sectional area (1.0 m$^2$) and f is a factor to account for the field line helicity given by [2]

$$f = (5 + \theta^2 + 6\theta^3)/(5 + \theta^2) \tag{6}$$

Equation (6) is an analytic fit to graphical data presented in Ref. [2] and has not been independently verified for the present experiment. Measurements of oxygen line ratios, Doppler broadening of Carbon III and the neutral charge exchange spectrum suggest a peak temperature of $T_e \sim T_i \sim 100$ eV corresponding

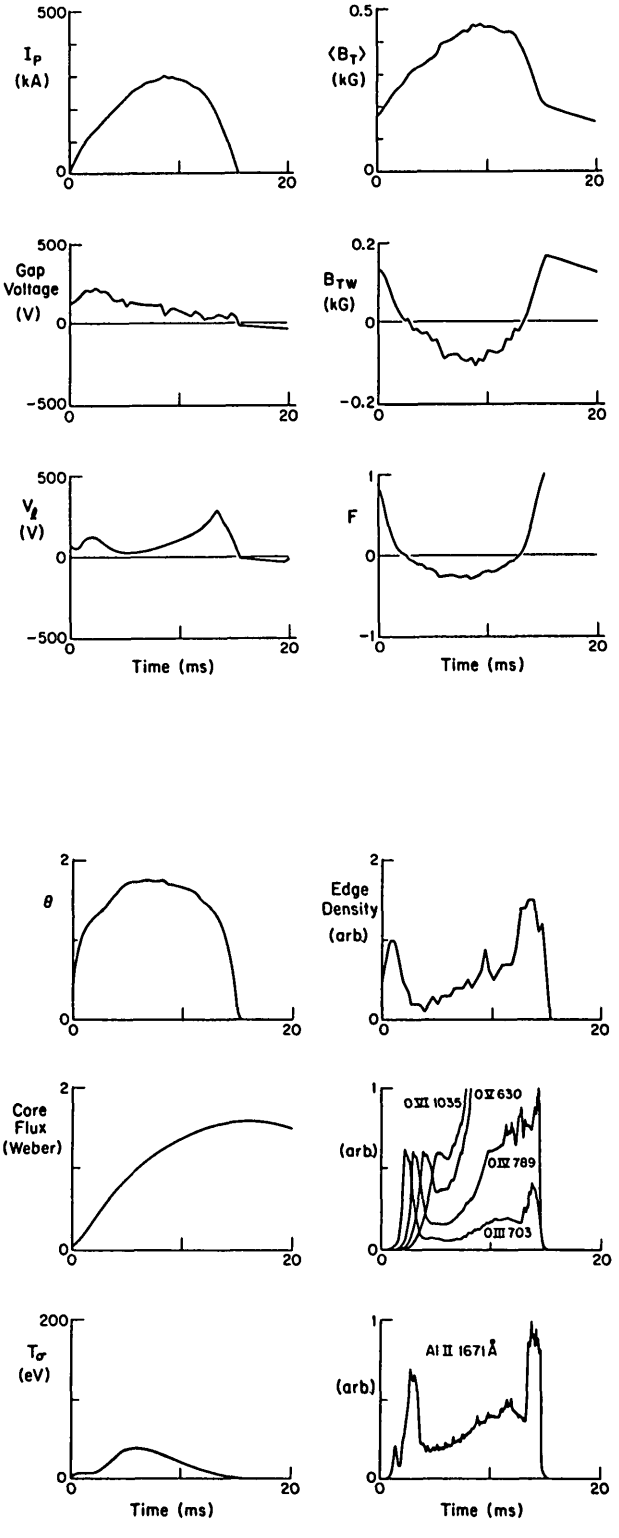


*FIG. 2. Time dependence of plasma current $I_p$, average toroidal magnetic field $\langle B_T \rangle$, Ohmic heating voltage at the electrical gap, toroidal field at the wall, toroidal loop voltage $V_\ell$, reversal parameter F, pinch parameter $\theta$, edge density n, flux in transformer core, oxygen impurity lines, conductivity temperature and aluminium impurity line.*

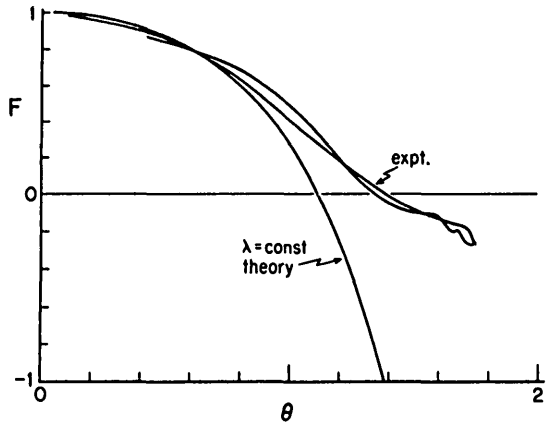


*FIG. 3. F–θ trajectory for a single experimental discharge and as theoretically predicted by a spatially constant-λ calculation for the non-circular boundary.*

to $Z_{eff} \sim 3$. From these parameters, one can calculate a global energy confinement time of $\sim 100\ \mu s$ at the time of the peak plasma current. One should be cautious not to interpret this time in terms of an RFP size scaling since the value is appropriate only to rather late in the discharge after a significant impurity influx has occurred and since there are a number of known, large magnetic field errors, particularly at the poloidal field voltage gap, that may be dominating the losses.

During a discharge the F–θ trajectory as shown in Fig. 3 lies to the right of the theoretical prediction. The prediction is based on a numerical calculation for a λ (= j/B) profile that is constant inside a region with the cross-sectional area as shown in Fig. 1.

In addition to examining the time evolution of a particular discharge, one can look at the properties of different discharges at a given time. Figure 4 shows 120 of the better discharges collected over a three month period with the data plotted at the time of the peak plasma current (typically, at 5–10 ms). The reversed field discharges have $\theta > 1.4$, and the tokamak ($q > 1$) discharges have $\theta < 0.4$. The current increases with θ up to $\theta \sim 1.1$ (non-reversed discharges) because the increase in θ is obtained by increasing the toroidal loop voltage. The current then

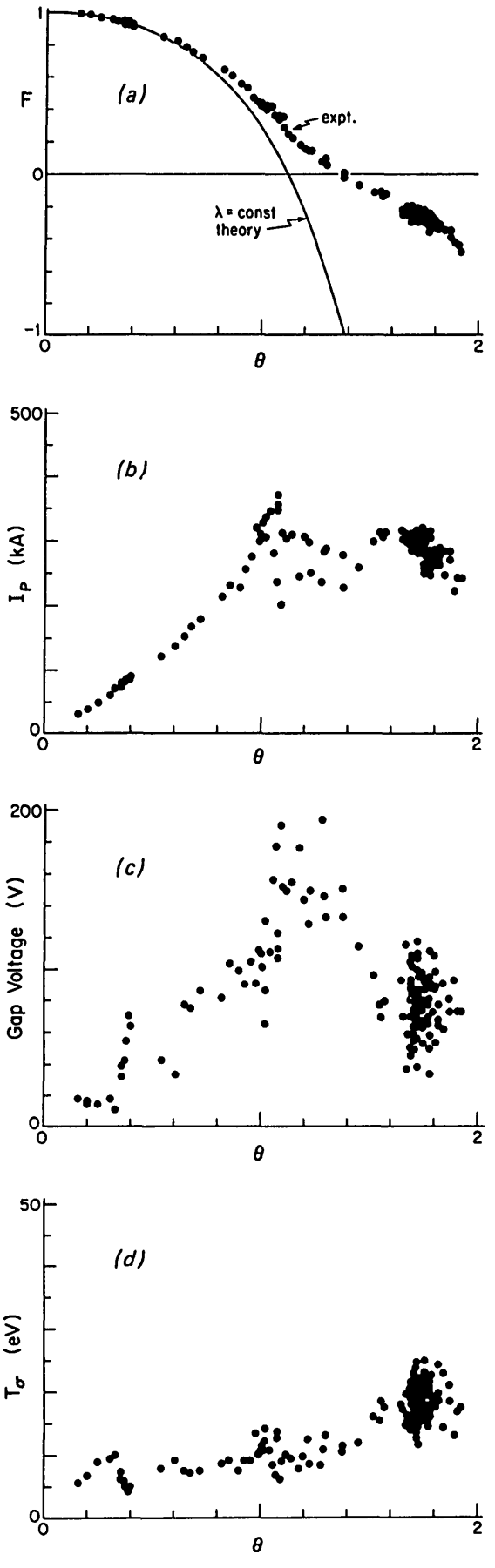


*FIG. 4. θ-dependence of field reversal parameter, plasma current, gap voltage and conductivity temperature obtained for 120 plasma discharges ranging from the $q > 1$ tokamak ($\theta < 0.4$) to the RFP regime ($\theta > 1.4$). The data are plotted at the time of the peak plasma current which is typically at 5–10 ms.*

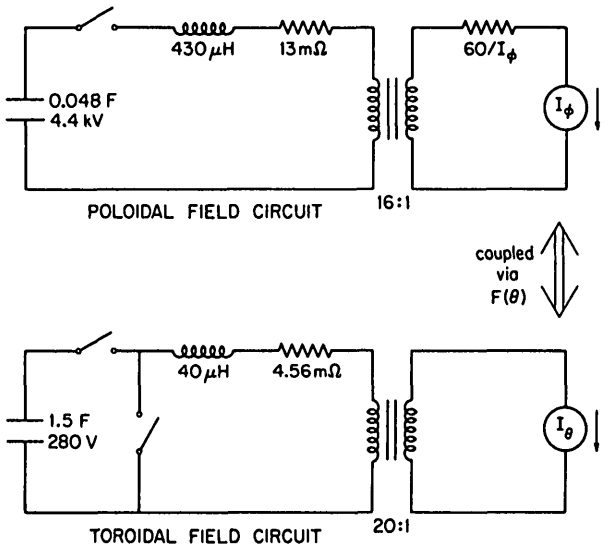


*FIG. 5. Electrical circuit used to model the time dependence of plasma electrical waveforms.*

decreases slightly, simply because the further increase in $\theta$ is obtained by a reduction in the toroidal magnetic field. The capacitor bank configuration prohibited further increase in loop voltage beyond that yielding $\theta \sim 1.1$. The RFP discharges have a lower loop voltage and higher conductivity temperature than the non-reversed discharges, but the fluctuation level is about the same for the two cases. The resistivity is somewhat higher than in other RFP plasmas at the same value of plasma current but perhaps not very different from those same devices run at a similar value of current density (300 $kA \cdot m^{-2}$) [8].

The experimentally observed electrical waveforms can be reproduced numerically [8–10] by the solution of the electrical circuit shown in Fig. 5. The poloidal and toroidal field circuits are coupled through the experimentally observed F–$\theta$ relation. The only other experimental input is the use of an empirically adjusted, time-independent loop voltage of 60 V in order to model the plasma resistance. The resulting agreement suggests that a plasma resistance that scales as $60/I_p$ for all conditions is a reasonable approximation. This circuit model has been useful for predicting the effect of various modifications to the electrical circuit.

Although the wall is indented, the indentation is not strong enough to produce an internal separatrix, as in the Multipinch [3]. Also, the transition to an up-down asymmetric state at high $\theta$, which occurs in the Multi-pinch experiment, is not seen in the present device.

TABLE I. PARAMETERS OF PLASMA USED FOR FLUCTUATION STUDIES

| | RFP | $q_a \sim 0.4$ | $q_a \sim 1.4$ |
|---|---|---|---|
| Plasma current (kA) | 175 | 275 | 120 |
| Startup voltage (V) | 160 | 220 | 140 |
| Average $B_T$ (G) | 350 | 620 | 750 |
| Toroidal voltage during sustainment (V) | 85 | 100 | 60 |

## 4. FLUCTUATION STUDIES

Fluctuation spectra have been investigated extensively on several reversed field pinch experiments [11]. To examine the influence of bad poloidal magnetic field curvature on stability, magnetic fluctuations have been measured in regions of good and bad curvature of the poloidal magnetic field for three different discharges. The three cases, described in Table I, include an RFP plasma and two non-reversed plasmas characterized by $q_a$, the edge safety factor (at r = a) for a circular plasma of equivalent area and current as in the present non-circular cases. The RFP and $q_a \sim 0.4$ plasmas have magnetic curvature dominated by that of the poloidal field, whereas at $q_a \sim 1.4$ the toroidal field curvature is stronger. The strength of the poloidal and toroidal curvature can be measured by the relative contributions to the total curvature vector $\vec{\kappa} = B^{-2} (\vec{B} \cdot \nabla)\vec{B}$. For a circular segment of magnetic surface, the ratio of poloidal curvature $\vec{\kappa_p} = B^{-2} (\vec{B} \cdot \nabla)\vec{B}_P$ to toroidal curvature $\vec{\kappa_T} = B^{-2} (\vec{B} \cdot \nabla)\vec{B}_T$ (where $\vec{B}_P$ and $\vec{B}_T$ are poloidal and toroidal magnetic fields) is given by $\kappa_P/\kappa_T \sim \epsilon/q^2$, where $\epsilon$ is the inverse aspect ratio. Thus, at $q_a \sim 1.4$ we have $\kappa_P/\kappa_T \sim 1/6$, whereas at $q_a \sim 0.4$ we find $\kappa_P/\kappa_T \sim 2$. The magnetic surfaces are similar in all three cases and contain outer surfaces which have good poloidal curvature at the midplane and bad poloidal curvature at the top and bottom, as indicated in Fig. 1.

Fluctuations have been measured along horizontal chords which extend from the wall to a magnetic surface which lies 20 cm from the wall in the top/bottom regions and 4 cm from the wall at the midplane. Magnetic pickup coils consist of three, small, orthogonal

loops with overlapping areas to measure the three field components at one location. The coils (typically 80 turns, 7.5 $mm^2$ cross-section) are wound on machinable ceramic forms and inserted within 0.127 mm thick, 4.76 mm diameter stainless steel tubes which are then covered by a 1.58 mm boron nitride heat shield.

The first significant feature is that the fluctuations are unusually large in all cases. The large amplitude is suspected to arise from extraneous effects, such as plasma–wall interactions or known magnetic field errors. Fluctuation properties were seen to have been influenced by field errors [12] or plasma positioning in HBTX-IA. Despite the enhanced amplitude, the fluctuations exhibit various interesting and significant features. It is striking that RFP sustainment (the 'dynamo effect') appears to persist in the presence of fluctuations as large as 50% ($\tilde{B}/B \sim 0.5$). All fluctuation magnitudes refer to a root mean square value obtained from a 3 ms time average.

An interesting dependence on $q_a$ is evident in the non-reversed discharges. At $q_a \sim 1.4$, the magnitude of the time derivative of the fluctuations ($\dot{\tilde{B}}$) is roughly independent of the poloidal curvature. To characterize the dependence of fluctuations on curvature, the normalized fluctuation level $\vec{b} = \dot{\tilde{B}}/B$ (where B is the equilibrium field at the wall) is measured in the bad and good regions of a magnetic surface. The ratio of bad curvature region fluctuations to good curvature region fluctuations, $b_{bad}/b_{good}$, is plotted in Fig. 6 versus radial distance (across magnetic surfaces) for each component of field. Numerically computed equilibria, with assumed current density profiles, were used to match good curvature points with bad curvature points on the same magnetic surface. It is seen in Fig. 6 that at $q_a \sim 1.4$, the poloidal and toroidal magnetic field fluctuations are roughly uniform along a magnetic surface (ratio ~1), but the radial component peaks in the bad curvature region.

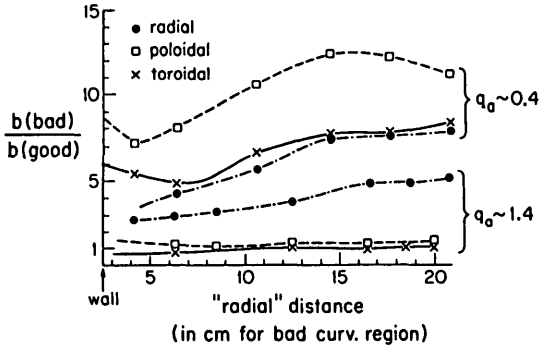


*FIG. 6. Curvature dependence of magnetic fluctuations for $q_a \sim 1.4$ and $q_a \sim 0.4$ plasmas. The ordinate is the ratio of fluctuation amplitude in the good curvature region to that in the bad curvature region of the same magnetic surface. $b = \dot{\tilde{B}}/B_W$ where $\dot{\tilde{B}}$ is the time differentiated fluctuation (rms), obtained from a 3 ms time average for $f < 300$ kHz, and $B_W$ is the equilibrium field at the wall. Profiles across magnetic surfaces ('radial') are obtained by horizontal magnetic probe scans in the midplane and top/bottom regions shown in Fig. 1. The abscissa labels the magnetic surface. The units indicate the distance of a surface from the wall as measured along a horizontal chord in the bad curvature region. The radial extent corresponds to about 10% of the total poloidal magnetic flux.*

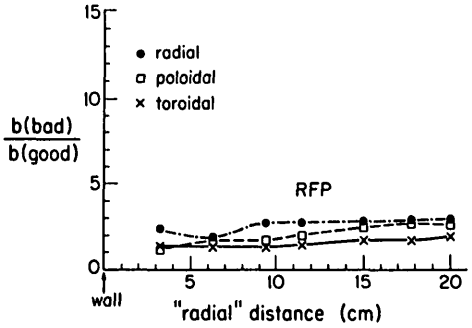


*FIG. 7. Curvature dependence of fluctuations in RFP plasmas. Data obtained as described for Fig. 6.*

For $q_a \sim 0.4$ non-reversed discharges, strong peaking of fluctuations in the bad curvature region is evident for all directional components, as shown in Fig. 6. Fluctuation levels in the bad curvature region typically exceed those in good curvature by a factor of five to ten. The onset of spatial peaking of the poloidal and toroidal field fluctuations as $q_a$ is lowered from 1.4 to 0.4 is consistent with the recognition that poloidal curvature becomes dominant at low $q_a$. In addition, if $q_a$ is less than one, the net curvature becomes unfavourable, and the plasma may be unstable to resistive interchange modes which might develop a ballooning character along a magnetic surface of non-uniform curvature.

For RFP discharges (Fig. 7) the fluctuations are roughly independent of curvature. This is a curious result since the poloidal curvature contribution to the total curvature is strongest for RFP discharges. This result suggests either that interchange modes contribute less to RFP turbulence than to turbulence in non-reversed ($q_a \sim 0.4$) pinches or that they are unable to localize (with resultant field line bending), perhaps a consequence of the increased magnetic shear of the RFP.

Finally, for all three cases studied there is a tendency for the fluctuations to be polarized perpendicular to the equilibrium field, along a magnetic surface. Such compressionless motion might be expected for a low beta plasma [13]. That is, at $q_a \sim 1.4$ the fluctuating field is nearly poloidal, at $q_a \sim 0.4$ it is oblique, and for RFP discharges it is nearly toroidal. The radial field fluctuation, $\tilde{B}_r$, is always several times smaller than the component within the magnetic surface.

## 5. MOVABLE LIMITER STUDIES

The unusually large cross-section and good access of the device allowed the installation of full toroidal rail limiters. Limiters in RFPs are of interest both for impurity control and for studying the effect on stability and sustainment of separating the plasma edge from a conducting boundary. The limiters were located at a major radius of 1.61 m on the lid and floor of the machine. They consisted of 2 mm thick, 3.1 cm wide, stainless steel with three, ceramic, insulating breaks. The lower limiter was fixed in position so that it extended 4.3 cm into the plasma, and the upper limiter was mounted on rods that allowed it to be inserted up to an additional 14 cm into the plasma. The limiters were electrically floating with respect to the machine wall.

Despite the insulating breaks, it was observed that a significant toroidal current (perhaps of the order of 1 kA) flowed in the limiters as evidenced by the fact that there were mechanical stresses which broke some of the insulators on the supports. There was also evidence of unipolar arcing on the limiter surface. The cause and consequences of this current are unknown.

Despite repeated attempts, it was not possible to get sustained RFP discharges with both limiters installed, even with the upper limiter retracted to within 4.3 cm of the wall. Consequently, the lower, fixed limiter was removed, leading to an inherent up-down asymmetry. With only the upper limiter, it was possible to obtain sustained discharges, although the plasma resistance was higher than it was without limiters.

Figure 8 shows the plasma current as a function of the limiter position, a, measured as a distance from the machine midplane to the limiter edge. The wall is at a position of 54 cm. These data were taken with the same poloidal bank voltage thus corresponding to an approximately constant toroidal loop voltage. When the limiter was inserted beyond the 40 cm point (14 cm from the wall), it became increasingly difficult to obtain sustained discharges at this voltage. A least square fit to the data shows that the plasma current varies approximately as the square of the distance of the limiter edge from the midplane. The simple interpretation is that the cross-sectional area of the plasma is shrinking while the plasma resistivity remains approximately constant.

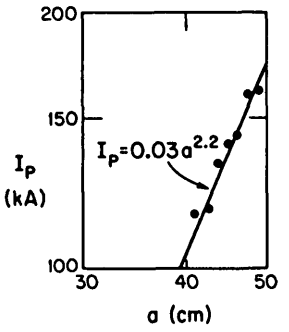


*FIG. 8. Variation of plasma current versus distance of the edge of the limiter from the midplane. The wall is at a = 54 cm. A least squares fit shows an approximate parabolic dependence.*

However, probe measurements near the wall in the outer midplane, about 90° poloidally away from the limiter, show that the density, electron temperature and magnetic field are not greatly affected by the presence of the limiter. For example, when the limiter is inserted, the reversal layer actually moves closer to the wall to within the shadow of the limiter. This motion towards the wall is consistent with the fact that F is closer to zero (the field is less deeply reversed) at the lower current values. The variation of the toroidal field near the wall implies that significant plasma current is present in the limiter shadow, and thus the limiting action is not effective. Hence, the inverse square dependence of plasma curent with distance to the limiter must be viewed as fortuitous. It is possible that large field errors are present near the wall or that the plasma has adjusted its equilibrium profile so that it touches the wall everywhere except in the immediate poloidal location of the limiter. On the basis of these tests, one cannot necessarily conclude that an RFP can successfully operate with toroidal limiters.

## 6. CONCLUSIONS

Sustainment beyond the plasma resistive diffusion time has been accomplished for an RFP plasma of large size and non-circular boundary. Parameters of the plasmas studied are, typically, $\langle a \rangle = 0.56$ m, $I = 250$ kA, $\tau_E \approx 0.1$ ms, and $T_e \sim T_i \sim 100$ eV.

The first wall exposed to plasma is the aluminium vacuum vessel (i.e. no stainless steel liner is used). The strength of the RFP sustainment mechanism (the 'dynamo') is further evident in that sustainment occurs in the presence of unusually large edge magnetic fluctuations ($\tilde{B}/B \sim 0.5$), presumably arising from extraneous effects such as large magnetic field errors which are known to be present.

Whereas circular RFP plasmas have bad curvature at all points along a magnetic surface, the present non-circular RFP contains both regions of good and bad curvature of the poloidal magnetic field (which is the dominant field component in the outer half of an RFP). Although good curvature is introduced in this configuration, it is expected [14] that the concomitant enhancement of the curvature in the bad curvature regions provides a slight net decrease in stability to pressure driven interchange modes. However, the non-uniform curvature may produce a non-uniformity (along a magnetic surface) in the amplitude of pressure driven instabilities. Thus, the spatial separation of good and bad curvature regions has allowed measurement of magnetic fluctuations as a function of curvature in order to address the issue of whether magnetic turbulence in RFPs is dominantly pressure or current driven. A further control in the experiment is the ability to operate as a tokamak-like, non-reversed pinch at both high edge safety factor ($q_a \sim 1.4$) as well as low ($\sim 0.4$). With high $q_a$ ($\sim 1.4$) and RFP discharges, the poloidal variation of the magnetic fluctuations is weak (except the radial component at $q_a \sim 1.4$). In contrast, at $q_a \sim 0.4$, the fluctuations are strongly peaked in the bad curvature regions. These results may be interpreted as follows: At $q_a \sim 1.4$, the toroidal curvature dominates so that poloidal variation of curvature-sensitive instabilities should be weak. Moreover, at $q > 1$, the net curvature is favourable, and interchange modes should be stable. At $q_a \sim 0.4$, the net curvature is bad, and interchange modes are likely to be unstable. The strong poloidal curvature domination provides strong localization of resistive interchange modes to the regions of local bad curvature. For RFP discharges, the poloidal curvature is strongest. The absence of fluctuation non-uniformity then implies that interchange mode contribution to RFP turbulence is relatively weak, as might be explained by the strong magnetic shear.

This device has also demonstrated two technological points relevant to an RFP reactor. Startup has been possible at relatively low toroidal loop voltages ($\lesssim 200$ V), an expected result of the large cross-sectional area (low resistance). In addition, operation with the electrical break (for application of toroidal loop voltage) exposed to the plasma, but protected by ceramic armour, has been demonstrated without arcing up to 300 V. Finally, RFP plasmas have been sustained with a toroidal limiter but with increased electrical resistance.

## ACKNOWLEDGEMENTS

The authors wish to thank John Laufenberg for his technical assitance, Professor D.W. Kerst for useful discussions, and Y.L. Ho for providing the numerical equilibria.

This work was supported by the US Department of Energy and the National Science Foundation.

## REFERENCES

[1] See, for example, the series of articles in Plasma Physics and Controlled Nuclear Fusion Research 1984 (Proc. 10th Int. Conf. London, 1984), Vol. 2, IAEA, Vienna (1985) 431 ff.

[2] BURTON, W.M., BUTT, E.P., COLE, H.C., GIBSON, A., MASON, D.W., PEASE, R.S., WHITEMAN, K., WILSON, R., in Plasma Physics and Controlled Nuclear Fusion Research (Proc. 1st Int. Conf. Salzburg, 1962), Nucl. Fusion Supplement, Part 3, IAEA, Vienna (1963) 903.

[3] LaHAYE, R.J., JENSON, T.H., LEE, P.S.C., MOORE, R.W., OHKAWA, T., Nucl. Fusion **26** (1986) 255.

[4] KERST, D.W., FORSEN, H.K., MEADE, D.M., et al., in Plasma Physics and Controlled Nuclear Fusion Research 1971 (Proc. 4th Int. Conf. Madison, 1971), Vol. 1, IAEA, Vienna (1972) 3.

[5] BAKER, D.A., BUCHENAUER, C.J., BURKHARDT, L.C., et al., in Plasma Physics and Controlled Nuclear Fusion Research 1984 (Proc. 10th Int. Conf. London, 1984), Vol. 2, IAEA, Vienna (1985) 439.

[6] TAYLOR, J.B., Phys. Rev. Lett. **32** (1974) 1139.

[7] SPITZER, L., Jr., HARM, R., Phys. Rev. **89** (1953) 977.

[8] SCHOENBERG, K.F., GRIBBLE, R.F., PHILLIPS, J.A., Nucl. Fusion **22** (1982) 1433.

[9] BEVIR, M.K., GRAY, J.W., in Reversed Field Pinch Theory (Proc. Workshop, Los Alamos, LA-8944-C, 1981) (1981) 176.

[10] JOHNSTON, J.W., Plasma Phys. **23** (1981) 187.

[11] See, for example, HUTCHINSON, I.H., MALACARNE, M., NOONAN, P., BROTHERTON-RADCLIFFE, D., Nucl. Fusion **24** (1984) 59; ANTONI, V., ORTOLONI, S., Plasma Phys. **25** (1984) 799; TAMANO, T., CARLSTROM, T., CHU, C., GOFORTH, R., JACKSON, G., LaHAYE, R., OHKAWA, T., SCHAFFER, M., TAYLOR, P.,

BROOKS, N., CHASE, R., in Plasma Physics and Controlled Nuclear Fusion Research 1982 (Proc. 9th Int. Conf. Baltimore 1982), Vol. 1, IAEA, Vienna (1983) 609.

[12] NOONAN, P.G., TSUI, H., NEWTON, A.A., Plasma Phys. Controll. Fusion **27** (1985) 1307.

[13] KADOMTSEV, B.B., Plasma Turbulence, Academic Press (1966).

[14] SKINNER, D.A., PRAGER, S.C., TODD, A.M.M., Bull. Am. Phys. Soc. **31** (1986) 1580.

(Manuscript received 25 March 1987
Final manuscript received 1 July 1987)